



Journal of Applied Sciences

ISSN 1812-5654

science
alert

ANSI*net*
an open access publisher
<http://ansinet.com>

Analysis of Fluid Flow of Urea in a Perforated Rotating Bucket: Single Orifice Case

Aadil Muhammad, Nejat Rahmanian and Rajashekhar Pendyala
Department of Chemical Engineering, Universiti Teknologi PETRONAS,
Bandar Sri Iskandar, 31750 Tronoh, Perak, Malaysia

Abstract: This study is focused on the breakup phenomenon of urea droplet jets emerging from the rotating prilling bucket by theoretical and computational methods. Urea melt is pumped into the perforated rotating bucket having different orifice sizes from which molten urea breaks out in the form of droplets and solidifies to form of prills. The breakup of liquid jet into droplets formation in the prilling process has been analyzed. The criteria of Ohnesorge and Weber number are used to determine the regime map for the droplet formation. By increasing the rotational speed, more secondary droplet are formed which are undesired in industrial process as it causes dust formation. Liquid viscosity and exit velocity are crucial parameters for prediction of droplet size distribution. Computational Fluid Dynamics simulation is used to find a more precise velocity of urea fluid and to confirm analysis of the droplet formation.

Key words: Break up modes, droplet size distribution, prilling, perforated rotating bucket

INTRODUCTION

The phenomenon of prilling is an important area of study due to the challenging factors such as the effects of surface tension on the droplet formation. Prilling is a granulation process (Rahmanian *et al.*, 2011) and it is the creation of solid prills by the growth of surface tension instabilities on the surface of liquid jets. Prilling is one of the most vital unit operations in fertilizer, pharmaceutical, food, magnesium, detergent and many other chemical industries. In urea prilling process, the urea melt is pumped into the perforated bucket which is installed at the top of the tower (Alamdari *et al.*, 2000). Then, bucket is rotated at high speed around its own vertical axis. As a result of centrifugal force the melt flows out of the perforations and curved liquid jets occur. Due to surface tension the liquid jets break down into droplets in spherical form. In urea prilling process the appearance, strength, flow ability, mechanical and physical properties of desired solid prills are important and can be improved by altering the parameters such as rotating speed, viscosity of molten fluid and orifice sizes (Rahmanian *et al.*, 1998). The process is also used to manage the sizes of the prills produced and to avoid the formation of secondary or satellite droplets which are undesired. The secondary drops can be a source of fines, dust explosion and lump formation (Gurney *et al.*, 2010). There is a need to optimize the rotating bucket to produce prills of the desired size in chemical industries.

It is hard to monitor the motion of the melt within the prilling bucket when molten liquid is flowing into the bucket. Earlier investigations have revealed that the final prills size is a function of breakage of liquid jet (Rayleigh, 1878).

Experimental and theoretical studies on the straight liquid jets break up have been widely carried out. Savart (1833), Rayleigh (1878) and Weber (1931) are the pioneers in the field of droplet formation for straight jets. A detailed review on straight jets is done by Eggers (1997). The study of break-up of curved jets is important as this breakup forms the basis of industrial prilling process. In urea prilling, urea melt is fed into the prilling bucket, which has the perforations on the wall surface (Rahmanian *et al.*, 2012). Due to the rotation of prilling bucket the urea melt flows out through the perforations which is shown in Fig. 1 (Wallwork *et al.*, 2001). The centrifugal force plays an important role for this phenomenon. Liquid jets flowing outwards from the perforations can be seen. Each jet is emerging from small orifices on curved face. Some of the breakup of jets can also be observed.

LITERATURE REVIEW

Various experiments has been done by Wong *et al.* (2004) using single orifice container. The container was rotated at different rotational speed. The velocity was assumed constant during experiments. High speed digital camera was used to capture the trajectory of jets. In the range of studied parameters four types of breakup modes

were recognized which named as M1, M2, M3 and M4. These are the four modes which describe the mechanism of breakup of liquid jets. The Ohnesorge number 'Oh' and Weber number 'We' are plotted in Fig. 2 indicating the different regimes, each of the mode have significant difference in break up process which is described in the following. In mode M1 primary droplets were formed very close to the orifice, having less or no secondary droplets. M1 is shown at low values of rotational speed and low velocity. Increasing the values of different parameters such as rotational speed and the size of orifice had caused formation of secondary droplets, which is called bi-modal drop size distributions and termed as M2. The mode M3 occurs by increasing the Oh number and moderate values of We number. In this mode, high exit velocity and high dynamic viscosity result in long thin ligaments of fluid between the primary drops which then distributed into many satellite droplets. The mode M4 is due to the large

swell disturbances which rupture back to orifice. This is an example of instability which is not focused. Here, the jet becomes shaky that it splits into small secondary or satellite droplets. The formation of this type of jets occurs at very low exit velocity and high viscosity. All of these modes are driven due to the disturbances along the liquid jet.

Figure 3 is reproduced here to show a view of jet breakup. It displays a clear view for the breakup of liquid jets in different modes. A pilot scale experiment to study the mechanism of the breakup of liquid jets was also conducted by Partridge *et al.* (2005). In their study only two modes M2 and M3 were recognized. M1 and M4 were not observed in the pilot scale. A major difference between the liquid curved jets and straight jets depends on the rotational speed of the container (Rahmanian *et al.*, 2013). The rotation speed affects the exits velocity, drop size, trajectory, break up length and wave length of disturbances developing on liquid jet surface compared to straight jets (Van't Land, 2005).



Fig. 1: A top view of the prilling bucket rotating anticlockwise (Wallwork *et al.*, 2001)

MATERIALS AND METHODS

There are significant attempts to model and predict the behaviour of the rotating bucket in prilling process (Wong *et al.*, 2004; Partridge *et al.*, 2005). Aluminium 6061T6 Alloy is used as the material of prilling bucket. The process is affected by physical and chemical properties of the feed material, process parameters and geometry of the bucket. Therefore, the model can be based on a number of factors such as rotational speed, properties of urea melt, arrangement of the orifice size and angle of trajectory. A prilling bucket model has been constructed based on the data in Table 1. The prilling bucket is prepared by using Catia software (V5R17). A three dimensional geometry of

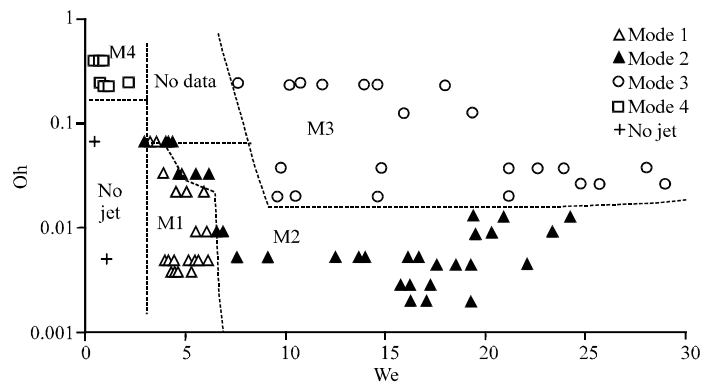


Fig. 2: Break-up regime map of Oh against We (Wong *et al.*, 2004)

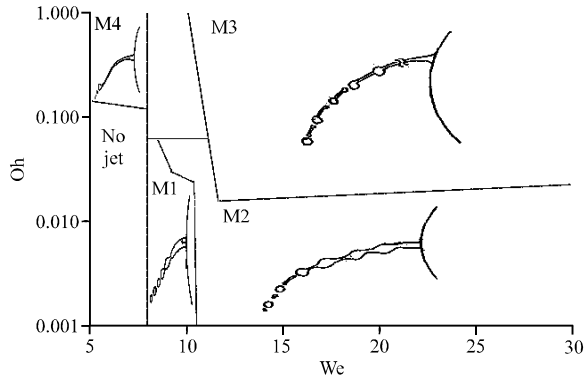


Fig. 3: Break-up sketches of Oh against We

Table 1: Data for the prilling bucket (Friestad, 1975)

Parameters	Values
Upper diameter for prilling bucket (mm)	150.0
Lower diameter for prilling bucket (mm)	80.0
Height (mm)	200.0
Orifice diameter for top row (mm)	3.8
Orifice diameter for bottom row (mm)	2.4
Number of orifice rows (-)	64.0
Orifices per row (-)	35.0
Total No. of orifices (-)	2240.0

perforated rotating bucket is shown in Fig. 4. Immense of outlet orifices can be clearly seen on the wall of the bucket.

Urea melt at above its melting point of 132°C is fed to the top of rotating prilling bucket. The bucket is rotated at high speed by the support of rotating shaft. Due to the centrifugal force, urea melt in the form of droplets falls out from the perforated wall of bucket. The main objective of this work is to determine the breakup modes of these droplets flowing out of the orifices. The angle along with every orifice is calculated to determine the radius at each point. The velocity of the droplet is calculated theoretically. We number is a dimensionless number and it is the ratio of kinetic energy to the surface tension given in Eq. 1:

$$We = \rho U^2 a / \sigma \tag{1}$$

It is important parameter which affects the flow of strongly curved surfaces and for the calculation of droplets and bubbles. Oh number indicates the influence of viscosity and is given in Eq. 2. It relates the viscous forces to inertial and surface tension forces:

$$Oh = \mu / \sqrt{\rho a \sigma} \tag{2}$$

We number and Oh number are calculated for all the orifices to check the behaviour of velocity and viscosity. The dimensionless numbers are then plotted as We against Oh.

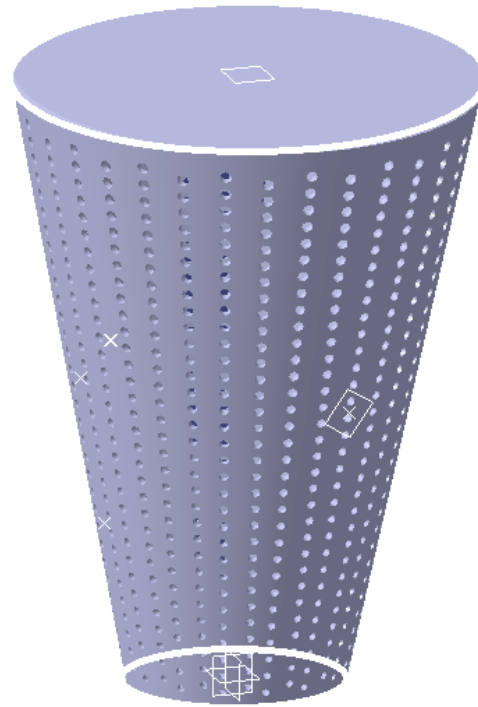


Fig. 4: Geometry of the prilling bucket

A CFD APPROACH

The use of Computational Fluid Dynamics (CFD) in this particular system is important to find the stable regime map. Computational fluid dynamics has been approached as a supportive means to study the process of spraying in the prilling bucket. Computational fluid dynamics can be named as virtual experiment as it represents the interface between experiments and theoretical studies (Yan *et al.*, 2012). It is also striking in many cases as it is more cost effective than the performing experiments (Ng *et al.*, 2009). The k-ε is most common model used for turbulence. In which variable "k" determines the energy in turbulence and "ε" is variable that determines the scale of turbulence. The governing equations which are used in k-ε model are shown in Eq. 3 and 4 (Bird *et al.*, 1963):

$$\frac{\partial}{\partial t}(\rho k) + \frac{\partial}{\partial x_i}(\rho k u_i) = \frac{\partial}{\partial x_j} \left[\left(\mu + \frac{\mu_t}{\sigma_k} \right) \frac{\partial k}{\partial x_j} \right] + G_k + G_b - \rho \epsilon - Y_M + S_k \tag{3}$$

And:

$$\frac{\partial}{\partial t}(\rho \epsilon) + \frac{\partial}{\partial x_i}(\rho \epsilon u_i) = \frac{\partial}{\partial x_j} \left[\left(\mu + \frac{\mu_t}{\sigma_\epsilon} \right) \frac{\partial \epsilon}{\partial x_j} \right] + C_{1\epsilon} \frac{\epsilon}{k} (G_k + C_{3\epsilon} G_b) - C_{2\epsilon} \rho \frac{\epsilon^2}{k} + S_\epsilon \tag{4}$$

Commercial software 'Ansys Fluent 14.0' is used for generating the results for three dimensional spraying

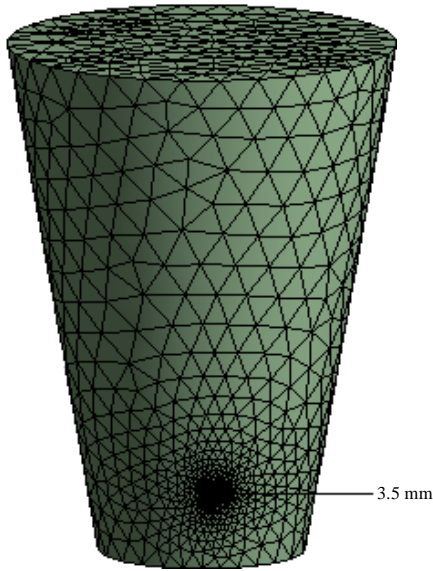


Fig. 5: Hexagonal mesh for single hole geometry in the rotating bucket

prilling bucket. Design modeller is used for creating the geometry of bucket having a single hole of 3.5 mm diameter. Simulation has been conducted with one hole to check the behaviour of flow regime. Mesh is generated with 7960 nodes by using sizing scheme of proximity and curvature. A simple solution method and first order scheme of pressure momentum is applied for the single orifice rotating bucket. Sensitivity analysis was done using different meshes such as triangular. However, for the cylindrical rotating geometry the orthogonal mesh was used as the final working mesh for CFD calculations as shown in Fig. 5. As the outlet orifice is the area of interest, so the mesh near the orifice is very fine for acquiring accurate results. To observe the flow behaviour, CFD has been run using cell zone and boundary conditions. As the bucket rotates so frame and rotational wall options are kept active in the software. The rotational speed is set at 630 rpm based on the patent data (Friestad, 1975). Atmospheric conditions are used on outlet where as the inlet mass flow rate is set to 31 ton h⁻¹.

RESULTS AND DISCUSSION

Figure 6 shows a schematic diagram of the rotating bucket. For schematic diagram dimensions are kept similar as those used in Catia model. To include the effect of orifice angle, theta (θ) is calculated at each orifice and then exit velocity of droplets at each orifice is calculated. Dimensional analysis is used to calculate Oh number and We number which are of great importance in identifying

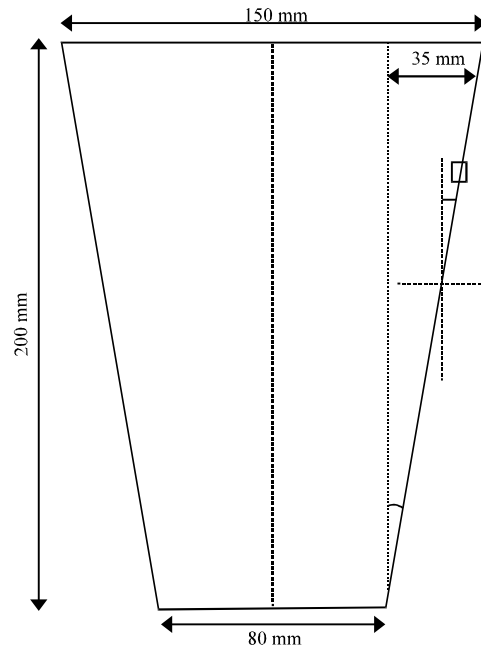


Fig. 6: Dimension of the prilling bucket

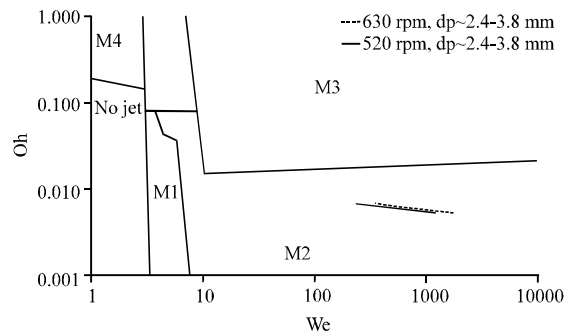


Fig. 7: Effects of rotational speed on the modes of operation in the prilling bucket

the break up mechanism. The calculated values of We against Oh are shown in Fig. 7 and 8. Different parameters such as rotational speed and orifice size are the variables. The data listed in Table 2 are used to calculate the We number and Oh number. Figure 7 shows the influence of rotation speed of bucket for the droplets in the range of 2.4-3.8 mm. The rotation speeds of 520 and 630 rpm are chosen. Both rotation speeds shows that under these conditions the droplet formation region falls under stable mode M2. By comparing Fig. 7 with regime map presented in Fig. 3, it is clearly seen that the operating modes of operation is M2. By increasing the orifice size and rotational speed, the formation of the undesired, secondary droplets occurs, results in a bi-modal size distribution of the droplets. This flow regime is indication of mode M2.

To investigate the effect of orifice size on the modes of breakup, We and Oh numbers were calculated under the constant rotational speed and size of orifices are

Table 2: Input data used in the calculation

Properties	Values
Dynamic viscosity μ ($\text{m}^{-2} \text{sec}$)	2.24×10^{-6}
Density ρ (kg m^{-3})	1247
Surface tension σ (N m^{-1})	66.3×10^{-3}
Orifice tension a (m)	2.4-3.8
Rotational speed Ω (rpm)	520-900
Jet velocity U (m sec^{-1})	2.79-4.94
Weber number (We)	0.0054-0.0068
Ohnesorge number (Oh)	351.90-1745.32

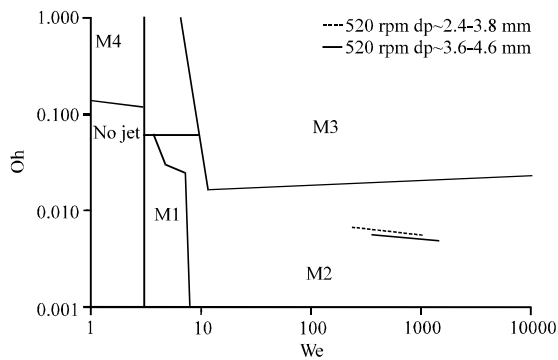


Fig. 8: Effects of orifice size on the modes of operation in the prilling bucket

altered. Figure 8 shows the results of this analysis. The droplet size is directly proportional to the We number. Increasing the orifice size is inversely proportional to Oh number as shown in Eq. 2. By changing the orifice size the regime map falls in mode M2, where the largest numbers of secondary droplets are formed.

In addition to simply identifying the mode of operation, the simulation results for the bucket containing single orifice are also discussed. CFD numerical simulation is conducted under steady state conditions with pressure based solver.

Figure 9 shows the streamline flow of melted urea on a plane at position of 24 mm from bottom in the bucket. Due to the presence of centrifugal force, urea melt is forced towards the wall and moving outwards from the outlet orifice. The vortexes observed in the streamlines are the proof that the bucket and fluid inside is rotating. The maximum and average outlet velocity obtained by CFD is 896 and 735 m sec^{-1} , respectively. The outlet velocity is observed to be very high and unrealistic as only one orifice is studied here, where as in actual geometry the numbers of holes are 2280. Figure 10 also shows a velocity profile showing the increase in velocity when fluid approaches at outlet orifice. It can be clearly observed that the velocity remain constant at plane but as the fluid arrive near the outlet orifice, velocity of fluid is increase abruptly. The Oh and We numbers are

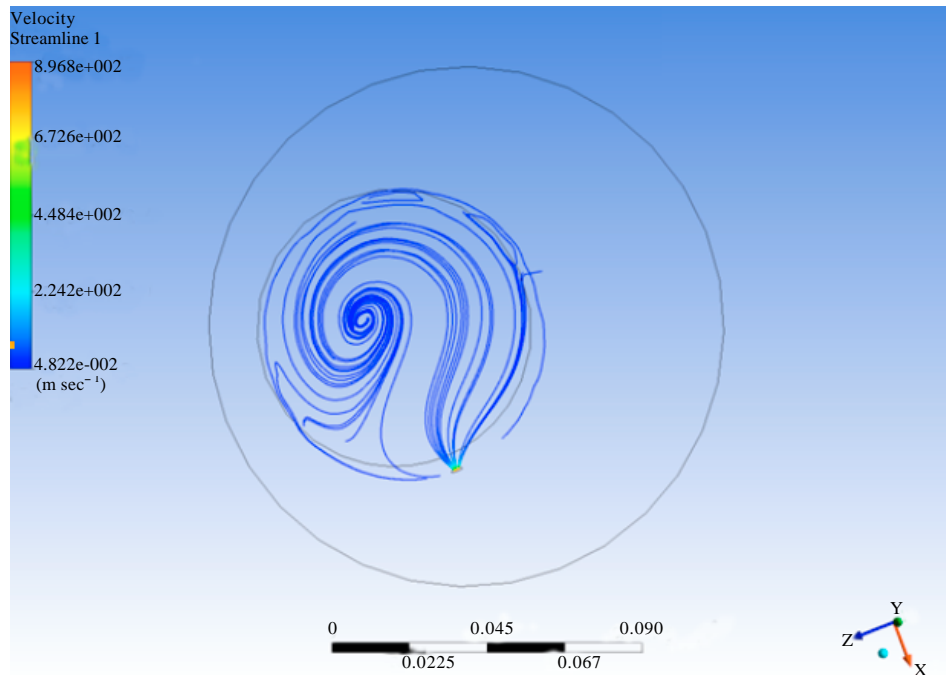


Fig. 9: Streamlines of urea melts in the rotating bucket containing single orifice

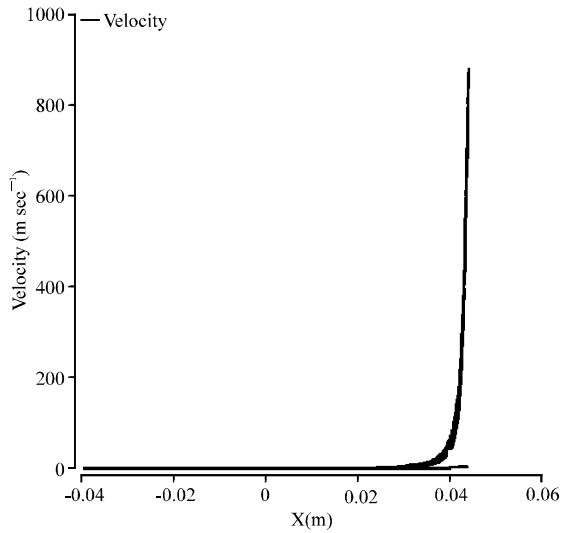


Fig. 10: Velocity profile at outlet plane in rotating bucket

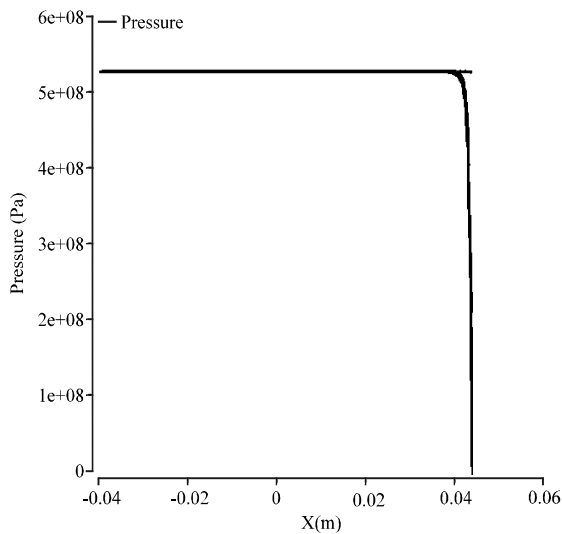


Fig. 11: Pressure profile at single orifice in rotating bucket

calculated by the average velocity calculated by CFD analysis. The breakup mode found by the regime map of We against Oh number tends to go from mode M2 to M3, in which ligaments starts producing and is not accepted to be an appropriate mode. Figure 11 shows the pressure profile in which sudden drop in pressure at the orifice profile is observed. This pressure is of course unrealistic for the real operating rotating bucket as in reality there is no bucket with single orifice in operation. In actual case, the pressure is break up among all orifices.

CONCLUSION

A parametric study has been carried out to investigate breakup of liquid jets produced in the rotating bucket and compare with a regime map available in the literature. The study showed that breakup length of jet is complex function for system parameters. Effects of different process parameters such as rotation speed and orifice size on the modes of operation were studied. Under the boundary of this study, for all cases the breakup of jet liquids falls in mode M2, where in addition to the primary droplets, satellite droplets are also formed. M2 breakup is the predicted for the generating accurate drop size forecast. In general, it is expected that more uniform particle size distribution is obtained by a more careful control of jet break-up results in the elimination of fines and proper transportation and bulk handling. This research is on going to study the influence of rotational speed on the velocity profile and droplet size distribution for a complete geometry of the rotating bucket which contains 2280 orifices.

ACKNOWLEDGMENT

Dr. N. Rahmanian would like to thank Universiti Teknologi PETRONAS for the financial support (Grant No.: STIRF 31/2011).

NOTATIONS

- a = Orifice radius, m
- D = Diameter, m
- Oh = Ohnesorge number
- p = Jet pressure, $\text{kg m}^{-1}\text{sec}^{-2}$
- t = Time, sec
- U = Jet exit velocity, m sec^{-1}
- We = Weber number
- μ = Dynamic viscosity, $\text{kg m}^{-1}\text{sec}^{-1}$
- ν = Kinematic viscosity, $\text{m}^2\text{sec}^{-1}$
- ρ = Density, kg m^{-3}
- σ = Surface tension, kg sec^{-2}
- ω = Frequency of disturbance
- Ω = Rotation rate, sec^{-1}

REFERENCES

- Alamdari, A., A. Jahanmiri and N. Rahmaniyan, 2000. Mathematical modelling of urea Prilling process. *Chem. Eng. Commun.*, 178: 185-198.
- Bird, R.B., W.E. Stewart and E.N. Lightfoot, 1963. *Transport Phenomena*. 2nd Edn., John Wiley and Sons, Singapore.

- Eggers, J., 1997. Nonlinear dynamics and breakup of free-surface flows. *Rev. Mod. Phys.*, 69: 865-930.
- Friestad, I.A., 1975. Means for feeding fluid material to a prilling bucket. United States Patent 3900164. <http://patent.ipexl.com/US/3900164.html>
- Gurney, C.J., M.J.H. Simmons, V.L. Hawkins and S.P. Decent, 2010. The impact of multi-frequency and forced disturbances upon drop size distributions in prilling. *Chem. Eng. Sci.*, 65: 3474-3484.
- Ng, B.H., Y.L.Ding and M. Ghadiri, 2009. Modelling of dense and complex granular flow in high shear mixer granulator-A CFD approach. *Chem. Eng. Sci.*, 64: 3622-3632.
- Partridge, L., D.C.Y. Wong, M.J.H. Simmons, E.I. Parau and S.P. Decent, 2005. Experimental and theoretical description of the break-up of curved liquid jets in the prilling process. *Chem. Eng. Res. Des.*, 83: 1267-1275.
- Rahmanian, N., A. Naji and M. Ghadiri, 2011. Effect of process parameters on the granule properties made in a high shear granulator. *Chem. Eng. Res. Design*, 89: 512-518.
- Rahmanian, N., M. Homavoonfard and A. Alamdari, 2012. Urea prilling process: Co-current vs Counter-current. Proceedings of the International Conference on Process, Environmental and Material Engineering, (PEME'12), Kuala Lumpur, Malaysia.
- Rahmanian, N., M. Homavoonfard and A. Alamdari, 2013. Simulation of urea prilling process: An industrial case study. *Chem. Eng. Commun.*, 200: 764-782.
- Rahmaniyan, N., A. Alamdari and A. Jahanmrrir, 1998. Modeling of the urea prilling tower. Proceedings of the 3rd World Congress on Particle Technology, Proceedings of the 3rd World Congress on Particle Technology, July 6-9, 1998, UK., pp: 94-100.
- Rayleigh, L., 1878. On the stability of jets. *Proc. Lond. Math. Soc.*, 10: 4-13.
- Savart, F., 1833. Memoire sur la constitution des veines liquides lancees par des orifices circulaires en mince paroi. *Ann. Chim., Phys.*, 53: 337-386.
- Van't Land, C.M., 2005. Industrial Crystallization of Melts. Marcel Dekker, USA.
- Wallwork, I.M., S.P. Decent, A.C. King and R.M.S.M. Schulkes, 2001. The trajectory and stability of a spiralling liquid jet. Part 1. Inviscid theory. *J. Fluid Mech.*, 459: 43-65.
- Weber, C., 1931. Zum zerfall eines flussigkeitsstrahles. *Z. Angew. Math. Mech.*, 11: 136-141.
- Wong, D.C.Y., M.J.H. Simmons, S.P. Decent, E.I. Parau and A.C. King, 2004. Break-up dynamics and drop size distributions created from spiralling liquid jets. *Int. J. Multiphase Flow*, 30: 499-520.
- Yan, Y., D. Guo and S.Z. Wen, 2012. Numerical simulation of junction point pressure during droplet formation in a microfluidic T-junction. *Chem. Eng. Sci.*, 84: 591-601.